Supplementary Information (SI) for Environmental Science: Nano.
This journal is © The Royal Society of Chemistry 2025

Supporting Information

MOF-derived Ni-Cu bimetallic interfaces synergy modified TiO_2 for efficient photocatalytic conversion of CO_2 to formate in ammonia nitrogen wastewater

Junjie Yang, [a] Jun Xie, [a, b] Junxian Qin, [a] Jin Shang, [c] Hiromi Yamashita, [d] Daiqi Ye, [a, e, f] Yun Hu*[a, e, f]

a School of Environment and Energy, South China University of Technology, Guangzhou 510006, P. R. China

b United Technology Center of Western Metal Materials Co., Ltd, Northwest Institute for Non-ferrous Metal Research, Shaanxi Institute for Materials Engineering, Xi'an, 710016 P. R. China

c Division of Materials and Manufacturing Science, Graduate School of Engineering, Osaka University, Osaka 565-0871, Japan

d School of Energy and Environment, City University of Hong Kong, Kowloon, 999077, Hong Kong

e Guangdong Provincial Key Laboratory of Atmospheric Environment and Pollution Control, Guangzhou 510006, P. R. China

f The Key Lab of Pollution Control and Ecosystem Restoration in Industry Clusters, Ministry of Education, Guangzhou510006, P. R. China

*Corresponding author. Phone: +86-20-3938-0569, E-mail: huyun@scut.edu.cn

1. Supporting Figures

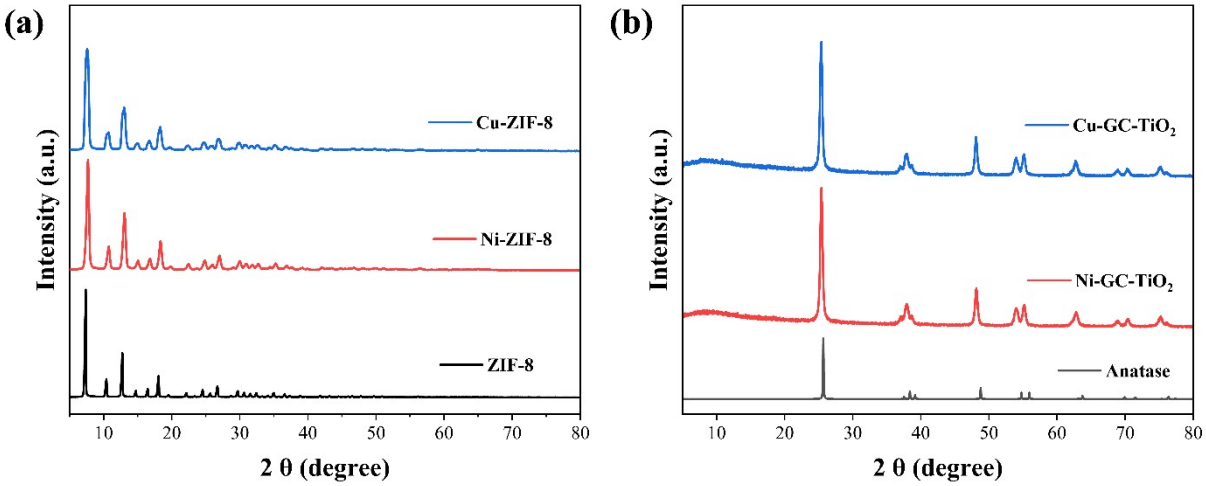

Fig. S1 XRD pattern of (a) single metal MOF precursor (b) single metal composite material.

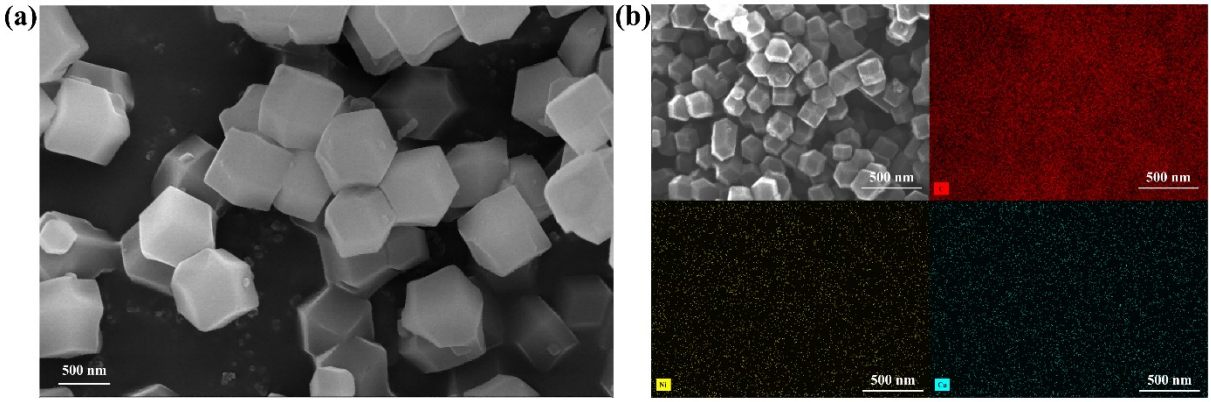

Fig. S2 (a) SEM pattern of ZIF-8 (b) EDS pattern of NiCu-GC.

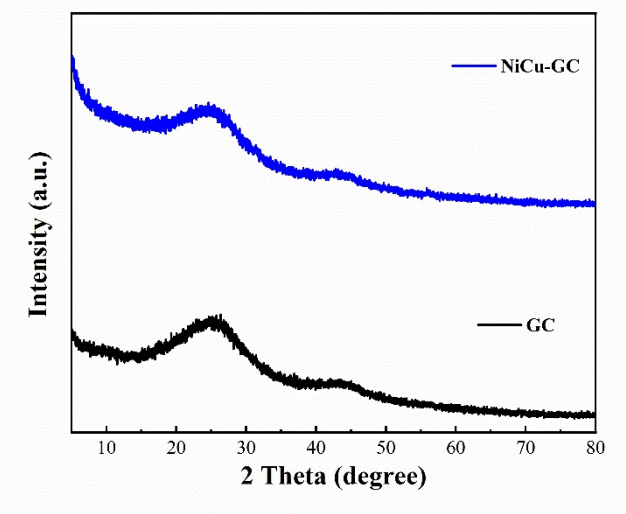

Fig. S3 XRD pattern of NiCu-GC.

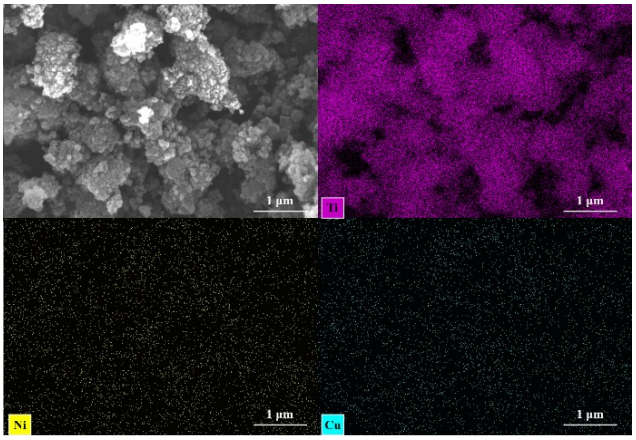

Fig. S4 EDS pattern of NiCu-GC-TiO_2.

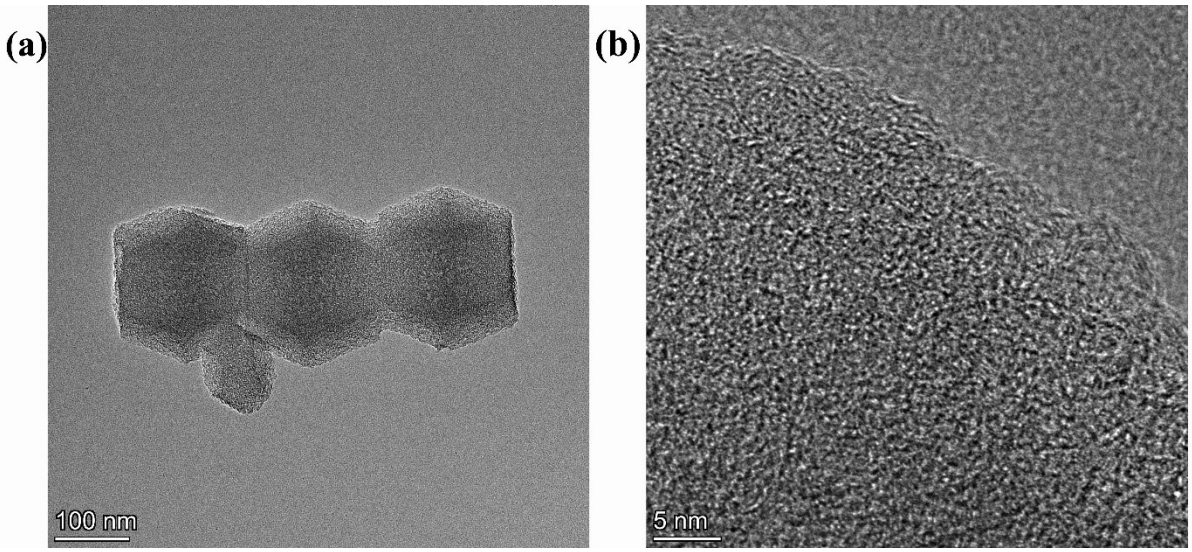

Fig. S5 TEM pattern of NiCu-GC.

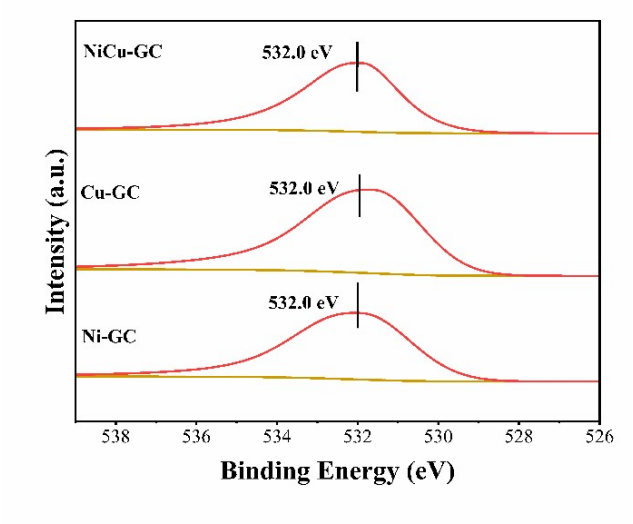

Fig. S6 XPS spectrums of derivatives O 1s.

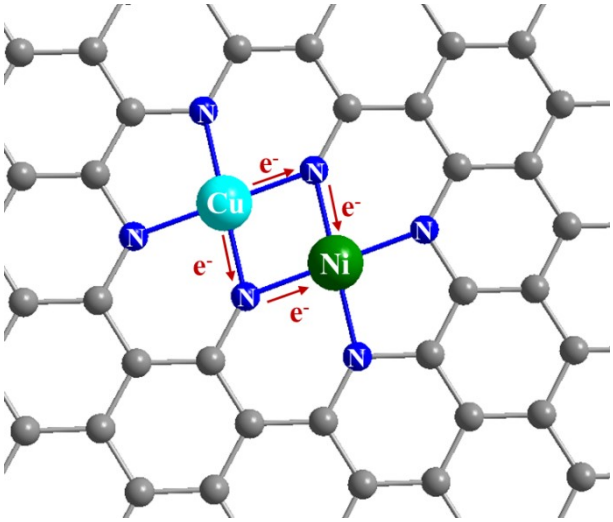

Fig. S7 Schematic diagram of the dual active sites in the NiCu-GC and the charge transfer situation.

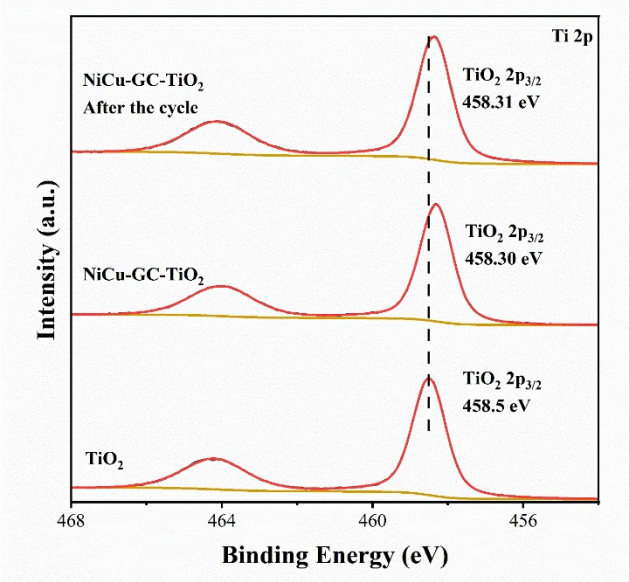

Fig. S8 XPS spectra of NiCu-GC-TiO_2 before and after cyclic reaction.

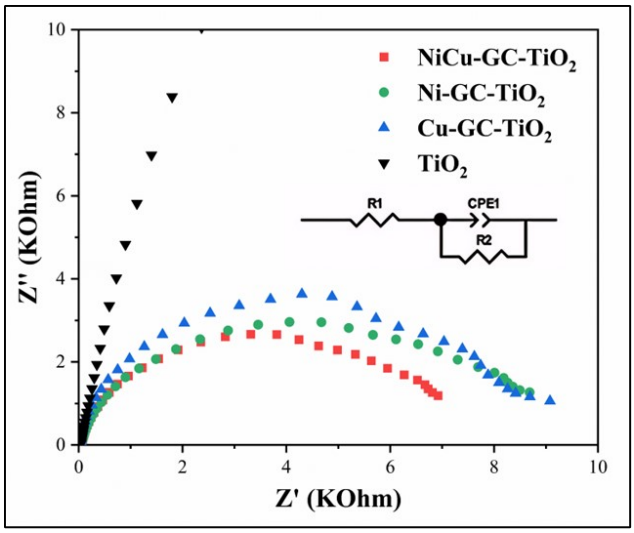

Fig. S9 The EIS plot of different materials.

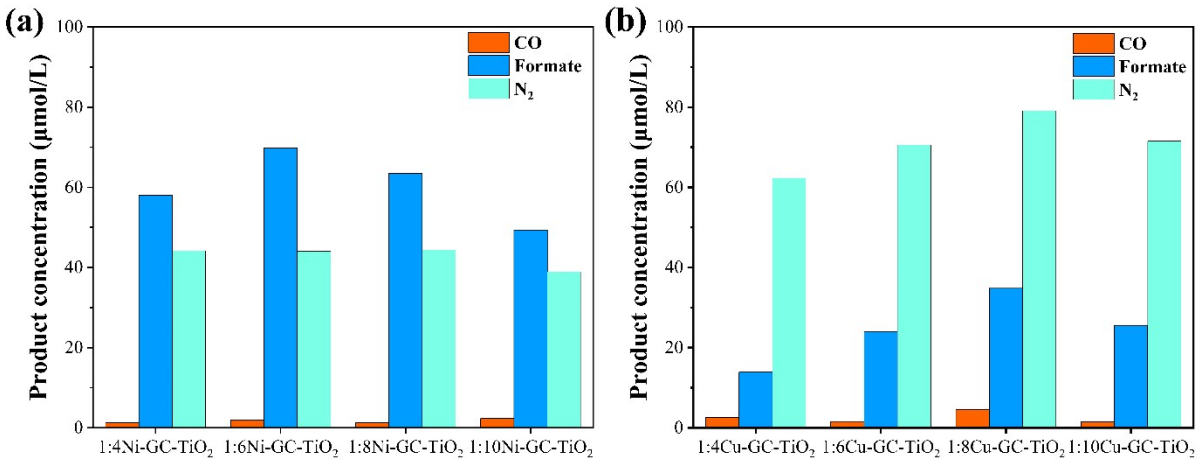

Fig. S10 Photocatalytic activity of (a) Ni doped materials with different ratios (b) Cu doped materials with different ratios.

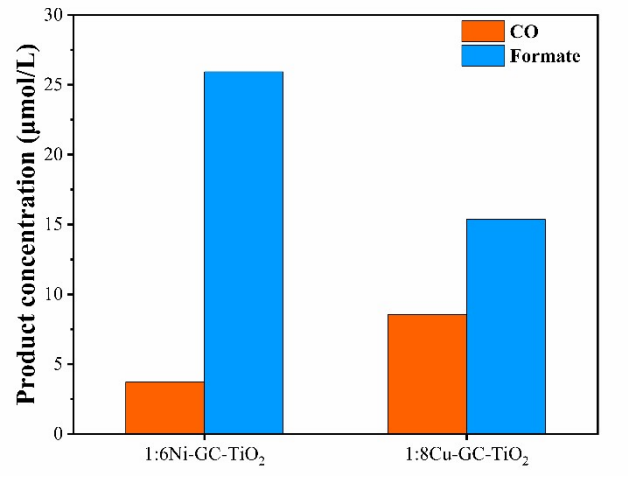

Fig. S11 Photocatalytic activity test of materials in pure water.

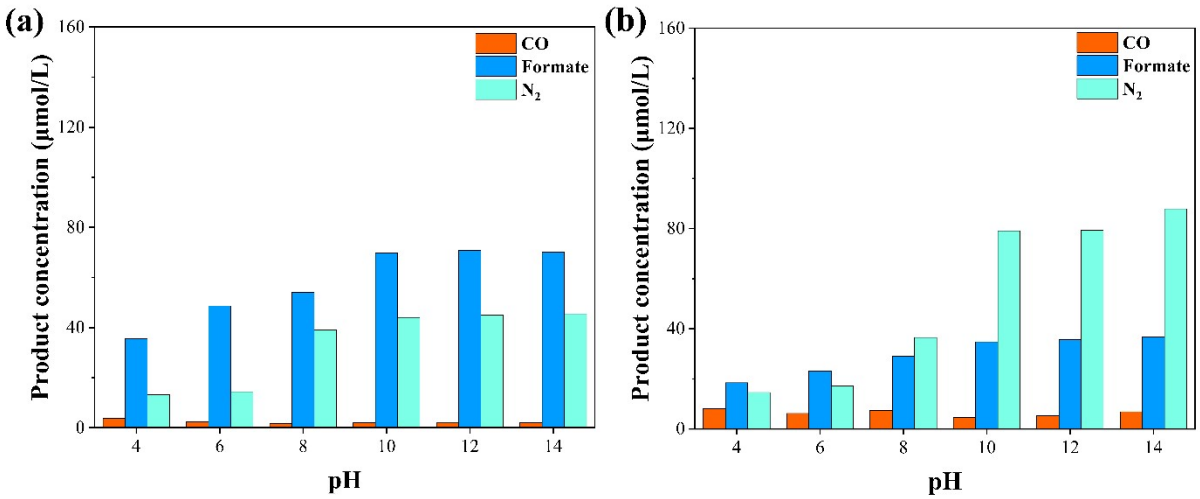

Fig. S12 Photocatalytic activity of (a) Ni-GC-TiO_2 (b) Cu-GC-TiO_2 at different pH.

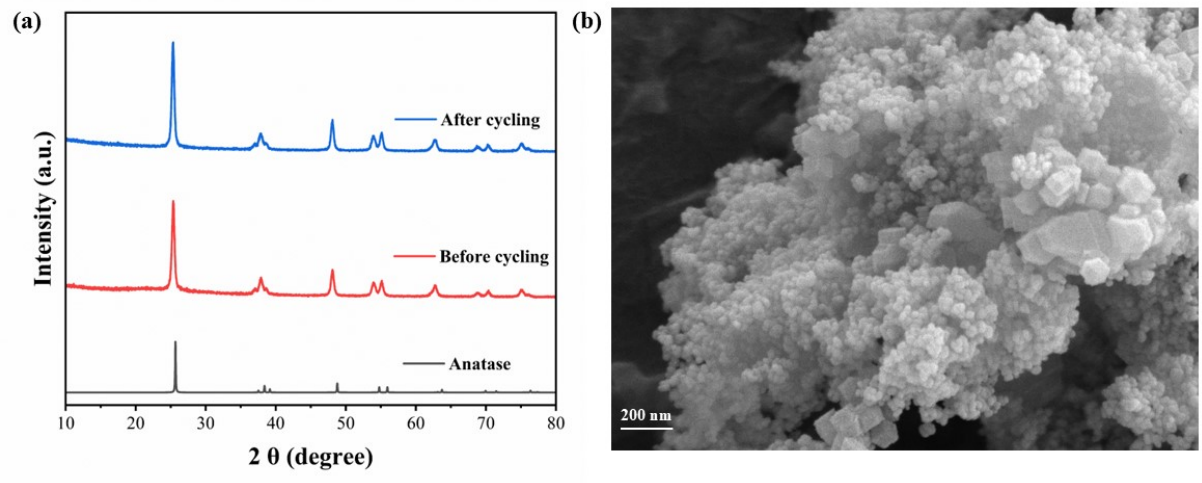

Fig. S13 (a) XRD pattern before and after cycling, (b) SEM image of the material after cycling.

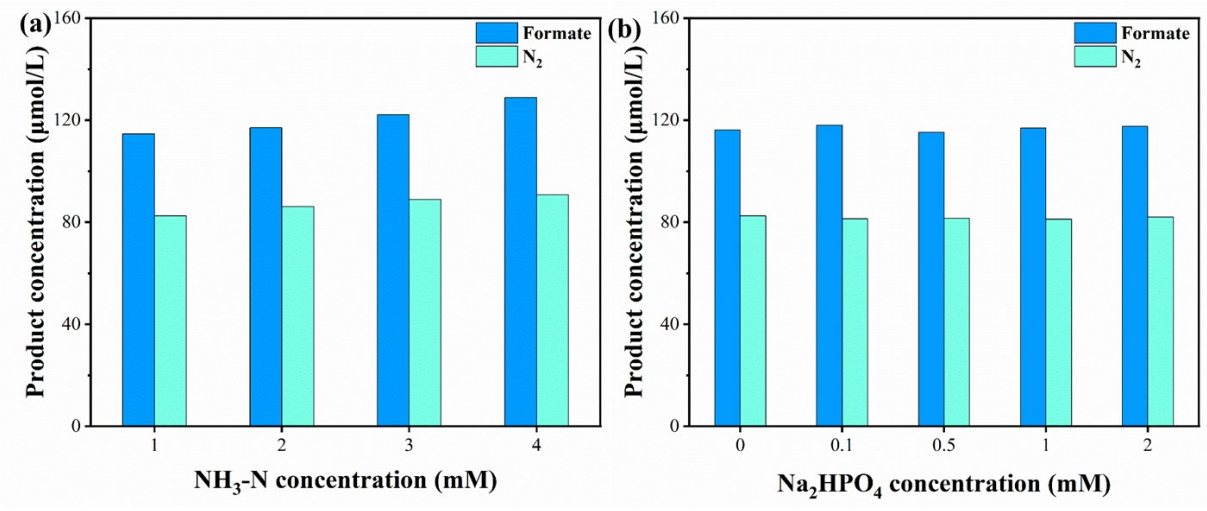

Fig. S14 Simulated wastewater photocatalytic activity test (a) different concentration of ammonia nitrogen (b) different concentration of sulphate

2. Supporting Tables

Table. S1 Ammonia nitrogen test results after different reaction durations.

Time (h)	NiCu-GC-TiO_2			Ni-GC-TiO_2			Cu-GC-TiO_2		
	NH_3 removal μmol/L	NO_2^- μmol/L	NO_3^- μmol/L	NH_3 removal μmol/L	NO_2^- μmol/L	NO_3^- μmol/L	NH_3 removal μmol/L	NO_2^- μmol/L	NO_3^- μmol/L
0.5	96.79	0.35	1.05	39.95	0.64	1.21	95.96	2.87	1.13
1	141.15	0.58	2.14	68.89	0.93	2.47	139.37	3.69	2.29
2	166.67	0.75	4.03	89.95	1.32	4.82	169.31	4.27	4.73
4	179.89	1.26	5.52	105.82	2.36	10.85	182.28	7.76	10.15
6	203.60	1.75	6.34	121.69	3.02	15.72	203.70	11.32	15.89
8	231.22	2.30	6.89	145.50	3.75	21.83	231.48	15.86	21.47
10	259.79	2.811	7.23	161.38	4.06	25.99	261.64	19.84	25.31
12	278.49	3.32	7.47	161.38	4.00	27.63	288.10	23.31	27.13

Table. S2 Cycle Test Comparison

Catalyst	Cycles times	Percentage of decline(%)	Ref.
NiCu-GC-TiO_2	5	1	This work
$V_{O,N}$-NBCN	5	~4	[1]
Cu_2O@MgO	5	~9	[2]
UiO-66(Ce)/BiOBr	5	14.7	[3]
12FLTC/BCN	5	14	[4]
CR-TiO_2	3	~10	[5]

Table. S3 The results for photocatalytic CO_2 reduction in recent literature.

Catalyst	Reaction condition	Product yield	Ref.
NiCu-GC-TiO_2	10 mL H_2O 1 mM NH_3-N	Formate 116.2 μM in 2 h	This work
$NiCo_2O_4$	2 mL H_2O 7.5 mg $[Ru(bpy)_3]Cl_2 \cdot 6H_2O$ 3 mL Acetonitrile 1 mL Triethanolamine	CO 10.5 mmol g^{-1} h^{-1}	[6]
CoNi-MOF	5 mL CH_3CN/H_2O (v/v=4:1) 0.43 mM $[Ru(phen)_3](PF_6)_2$ 0.43 M Triethanolamine	CO 1.16 mmol g^{-1} h^{-1}	[7]
KGF-10	4 mL DMSO 0.1 M BIH	Formate 58.8 μmol in 5 h	[8]
CTF-BP	10 mL H_2O 30 mL Acetonitrile 10 mL Triethanolamine	CO 4.60 μmol g^{-1} h^{-1} CH_4 7.81 μmol g^{-1} h^{-1}	[9]
NiCo-TiO_2	50 mL H_2O 0.1 M Na_2SO_3 0.2 M CsOH	CH_3COOH 22.6 μmol g^{-1} h^{-1}	[10]
$Ni(pbi)(pyS)_2$	2 mL MeCN/ H_2O 2 mM eosin Y 400 mM TEOA	Formate ~98 μmol in 6h	[11]
Cu–NH_2-MIL-125	18 mL Acetonitrile 2 mL TEOA	Formate 15.6μmol g^{-1} h^{-1}	[12]
$Cu_{0.05}Zn_{2.95}In_2S_6$ @CQDs-T	50 mL H_2O/CH_3CN/TEOA (v/v/v=1:3:1) 16.5 mg $[Ru(bpy)_3]Cl_2 \cdot 6H_2O$	CO 70.69 μmol g^{-1} h^{-1}	[13]

Supporting References

1. J. Jiang, X. Wang, Q. Xu, Z. Mei, L. Duan and H. Guo, Understanding dual-vacancy heterojunction for boosting photocatalytic CO_2 reduction with highly selective conversion to CH_4, *Applied Catalysis B: Environmental*, 2022, **316**, 121679.
2. J. Shi, A. Wang, Y. An, S. Chen, C. Bi, L. Qu, C. Shi, F. Kang, C. Sun, Z. Huang, H. Qi and J. Hu, Core@shell-structured catalysts based on Mg-O-Cu bond for highly selective photoreduction of carbon dioxide to methane, *Advanced Composites and Hybrid Materials*, 2023, **7**, 2.
3. H. Zhang, J. Ye, Y. Dai, H. Yang, J. Zhang, Y. Xie and W. Zhang, Ce^{4+}/Ce^{3+} redox effect-promoted UiO-66(Ce)/BiOBr heterojunction for enhancement photoreduction CO_2 under visible light, *Chemical Engineering Journal*, 2024, **502**, 158240.
4. H. Wang, Q. Tang and Z. Wu, Construction of Few-Layer Ti_3C_2 MXene and Boron-Doped g-C_3N_4 for Enhanced Photocatalytic CO_2 Reduction, ACS Sustainable Chemistry & Engineering, 2021, **9**, 8425-8434.
5. Z. Wang, L. Ma, B. Chen, Y. Zhang, K. H. Wong, W. Zhao, C. Wang, G. Huang and S. Xu, A green and efficient strategy to utilize spent SCR catalyst carriers: in situ remediation of Cu@TiO_2 for photocatalytic hydrogen evolution, *Green Chemistry*, 2025, **27**, 240-247.
6. B. Han, J. Song, S. Liang, W. Chen, H. Deng, X. Ou, Y.-J. Xu and Z. Lin, Hierarchical $NiCo_2O_4$ hollow nanocages for photoreduction of diluted CO_2: Adsorption and active sites engineering, *Applied Catalysis B: Environmental*, 2020, **260**, 118208
7. J. Zhang, Y. Wang, H. Wang, D. Zhong and T. Lu, Enhancing photocatalytic performance of metal-organic frameworks for CO_2 reduction by a bimetallic strategy, *Chinese Chemical Letters*, 2022, **33**, 2065-2068.
8. Y. Kamakura, C. Suppaso, I. Yamamoto, R. Mizuochi, Y. Asai, T. Motohashi, D. Tanaka and K. Maeda, Tin(II)-based metal–organic frameworks enabling efficient, selective reduction of CO_2 to formate under visible light, *Angewandte Chemie International Edition*, 2023, **62**, e202305923.
9. J. Li, P. Liu, H. Huang, Y. Li, Y. Tang, D. Mei and C. Zhong, Metal-free 2D/2D black phosphorus and covalent triazine framework heterostructure for CO_2 photoreduction, *ACS Sustainable Chemistry & Engineering*, 2020, **8**, 5175-5183.
10. G. Jia, M. Sun, Y. Wang, Y. Shi, L. Zhang, X. Cui, B. Huang and J. C. Yu, Asymmetric coupled dual-atom sites for selective photoreduction of carbon dioxide to acetic acid, *Advanced Functional Materials*, 2022, **32**, 2206817.
11. S. E. Lee, A. Nasirian, Y. E. Kim, P. T. Fard, Y. Kim, B. Jeong, S.-J. Kim, J.-O. Baeg and J. Kim, Visible-light photocatalytic conversion of carbon dioxide by Ni(II) complexes with N4S2 coordination: Highly efficient and selective production of formate, *Journal of the American Chemical Society*, 2020, **142**, 19142-19149.
12. A. Pancielejko, M. A. Baluk, H. Zagórska, M. Miodyńska-Melzer, A. Gołąbiewska, T. Klimczuk, M. Krawczyk, M. Pawlyta, K. Matus, A. Mikolajczyk, H. P. Pinto, A. Pieczyńska, J. Dołżonek and A. Zaleska-Medynska, Cu-incorporated NH_2-MIL-125(Ti): a versatile visible-light-driven platform for enhanced photocatalytic H_2 generation and CO_2 photoconversion, *Materials Horizons*, 2025, **12**, 957-972.
13. J. Yang, Y. Hou, J. Sun, J. Wei, S. Zhang, J. Liang, Z. Yu, H. Zhu and S. Wang, Corn-straw-derived,

pyridine-nitrogen-rich NCQDs modified $Cu_{0.05}Zn_{2.95}In_2S_6$ promoted directional electrons transfer and boosted adsorption and activation of CO_2 for efficient photocatalytic reduction of CO_2 to CO, *Chemical Engineering Journal*, 2023, **472**, 145142.